Pitch-variable blazed grating consisting of freestanding silicon beams

doi: 10.1364/OE.17.004419

Pitch-variable blazed grating consisting of freestanding silicon beams

Yongjin Wang*, Yoshiaki Kanamori, and Kazuhiro Hane*

Department of nanomechanics, Tohoku University, Sendai 980-8579, Japan
**Corresponding author:wang@hane.mech.tohoku.ac.jp, hane2@hane.mech.tohoku.ac.jp*

Abstract: Theoretical analysis is presented for a pitch-variable blazed grating which consists of freestanding silicon beams. The pitch-variable blazed grating is implemented by combining silicon-on-insulator (SOI) technology with microelectronicmechanical system (MEMS) technology. The whole device is fabricated on a 10μm silicon device layer to guarantee sufficient stiffness. The 4-level blazed surface profile is realized by combining a two-mask process with fast atom beam etching. Electrostatic combdrive microactuators with double folded springs are proposed to stretch the freestanding grating beams. In association with reactive ion etching and vapor HF release, the freestanding grating beams and the microactuators are obtained, and a Cr/Au film is deposited onto the blazed grating surfaces by a protective mask process to improve the diffracted power. Mechanical response and diffraction efficiency of fabricated devices are characterized, and the experimental results indicate that the fabricated 4-level blazed gratings extend both the tuning range and the diffraction efficiency of the 1st diffraction order of present MEMS diffraction gratings.

OCIS codes: (220.4241) Nanostructure fabrication; (230.5298) Photonic crystal; (260.5740) Resonance.

References and links

1. H. Sagberg, M. Lacolle, I.-R. Johansen, O. Løvhaugen, R. Belikov, O.Solgaard, and A. Sudbø, "Micromechanical gratings for visible and near-infrared spectroscopy," IEEE J. Sel. Topics Quantum Electron.**10**, 604 (2004).
2. A.Q. Liu and X.M. Zhang, "A review of MEMS external-cavity tunable lasers," J. Micromech. Microeng. **17**, R1 (2007).
3. C. Antoine, X. Li, J. Wang, and O. Solgaard, "Reconfigurable Optical Wavelength Multiplexer Using a MEMS Tunable Blazed Grating," J. Lightwave Technol. **25**, 3100 (2007).
4. J. Hsieh, S. Hsiao, H. Yin, W. Chen, C. Weng, Y. Lin, W. Fang, and K. Shieh, "An in-plane dispersive system utilizing micro tunable vertical grating," 2005 IEEE/LEOS International Conference on Optical MEMS and Their Applications Conference, pp.97-98.
5. W. Shih, S. Kim, and G. Barbastathis, "High-resolution electrostatic analog tunable grating with a single-mask fabrication process," J. Microelectromech. Syst. **15**, 763 (2006).
6. A. Q. Liu, B. Zhao, F. Chollet, Q. Zou, A. Asundi, and H. Fujita, "Micro-opto-mechanical grating switches," Sensors and Actuators A **86**, 127 (2000).
7. D. Yan and A. Lal, "Design and characterization of slit variable micrograting," IEEE J. Sensors. **6**, 458 (2006).
8. X. M.Zhang, Q. W.Zhao, T. Zhong, A. B. Yu, E. H. Khoo, C. Lu, and A. Q. Liu, "Variable nano-grating for tunable filters," 2007 Solid-state sensors, actuators and Microsystems conference, pp. 2417-2420.
9. M. Tormen, Y.-A. Peter, Ph. Niedermann, A. Hoogerwerf, and R. Stanley, "Deformable MEMS grating for wide tunability and high operating speed," J. Opt. A: Pure and Appl. Opt. **8**, 337 (2006).
10. X. Li, C. Antoine, D. Lee, J.-S. Wang, and O. Solgaard, "Tunable blazed gratings," J. Microelectromech. Syst. **15**, 597 (2006).
11. Y.-S. Yang and C.-H. Liu, "Design and fabrication of pitch tunable blaze grating," Proceeding of SPIE Photonics West 2005, Volume 5717 MEMS/MOEMS Components and Their Applications II -13.
12. Y.-C. Tung and K. Kurabayashi, "Nanoimprinted strain-controlled elastomeric gratings for optical wavelength tuning," Appl. Phys. Lett. **86**, 161113 (2005).
13. H. Tamada, "Blazed GxLPTM light modulators for laser projectors," J. Soc. Inf. Display **15**, 817 (2007).

#105846 - $15.00 USD Received 6 Jan 2009; revised 20 Feb 2009; accepted 26 Feb 2009; published 4 Mar 2009

14. M. W. Kowarz, J. C. Brazas, Jr., and J. G. Phalen, "Conformal grating electromechanical system (GEMS) for high-speeddigital light modulation," 2002 The Fifteenth IEEE International Conference on Micro Electro Mechanical Systems, pp.568-573.
15. S. K Yun, "Spatial optical modulator (SOM): Samsung's light modulator for next-generation laser displays," J. Soc. Inf. Display **15**, 321 (2007).
16. T. Shiono, T. Hamamoto, and K. Takahara, "High-efficiency blazed diffractive optical elements for the violet wavelength fabricated by electron beam lithography, " Appl. Opt. **41**, 2390 (2002).
17. M. Okano, H. Kikuta, Y. Hirai, K. Yamamoto, and T. Yotsuya, "Optimization of diffraction grating profiles in fabrication by electron beam lithography," Appl.Opt. **43**, 5137 (2004).
18. T. W. Ang, G. T. Reed, and A. Vonsovici, "Highly efficient unibond silicon-on-insulator blazed grating couplers," Appl. Phys. Lett. **77**, 4214 (2000).
19. C. Lee, K. Hane, and S. Lee, "The optimization of sawtooth gratings using RCWA and its fabrication on a slanted silicon substrate by fast atom beam etching," J. Micromech. Microeng. **18**, 45014 (2008).
20. M. Ahn, R. K. Heilmann, and M. L. Schattenburg, "Fabrication of ultrhigh aspect ratio freestanding gratings on silicon-on-insulator wafers," J.Vac.Sci.Technology. **B25**, 2593 (2007).
21. C.-h. Chang, R. K. Heilmann, R. C. Fleming, J. Carter, E. Murphy, T. C.Bailey, J. G. Ekerdt, R. D. Frankel, and R. Voisin, "Fabrication of sawtooth diffraction gratings using nanoimprint lithography," J.Vac.Sci.Technol.B **21**, 2755 (2003).
22. Y. Wang, Y. Kanamori, T. Sasaki, and K. Hane, "Design and fabrication of freestanding pitch-variable blazed gratings on silicon-on-insulator wafer," accepted by J. Micromech.Microeng.
23. S. Sinzinger and J. Jahns *Microoptics* (Wiley-VCH 1999).
24. Z. Jaroszewicz, A. Kolodziejczyk, A. Kowalik, and R. Restrepo, "Determination of phase-step errors of kinoform gratings from their diffraction efficiences," Opt. Eng. **40**, 692 (2001).

1. Introduction

Diffraction gratings are commonly used in optical components [1, 2, 3], which split light into several beams travelling in different directions. To tune light through diffraction, microelectronicmechanical systems (MEMS) are a promising solution. Several wavelength-tunable MEMS gratings have been developed for various applications [4-12]. There has also been substantial industrial R&D on high-efficiency MEMS gratings; specific examples include the following technologies: Sony GxL, Kodak GEMS and Samsung SOM [13, 14, 15]. On the other hand, high diffraction efficiency is important for diffraction gratings used in the field of telecommunication and spectroscopy. In order to obtain high output, diffraction gratings with a blazed surface profile have been reported by using dose-variable electron beam lithography [16, 17] and angle-controllable etching [18, 19]. However, the fabrication processes for these passive devices are costly and time consuming. Anisotropic etching in silicon has also been developed for generating a blazed surface profile with a fixed angle of 54.7° [10, 20], and a special nanoimprint lithography is also reported to fabricate 200nm period gratings with a 7° blazed angle for X-ray telescopes [21]. For our first-generation silicon blazed grating, the reflected output is found to be limited, and complicated interference in the silicon device layer also influenced the diffraction properties [22]. Moreover, since the pitch-variable grating was not analyzed theoretically, the general properties and limits of the proposed grating were not fully revealed.

This paper analyzes a pitch-variable blazed grating comprised of freestanding silicon beams with a blazed surface. The pitch-variable blazed grating is implemented by combining a silicon-on-insulator (SOI) technology with MEMS technology. The 4-level blazed surface profile is defined by a two-mask process, and top silicon is etched by fast atom beam (FAB) to generate the high lateral resolution. In association with reactive ion etching (RIE) and vapor HF release, the freestanding grating beams and MEMS actuators are realized on a 10μm silicon device layer, which can provide sufficient stiffness to the whole device. A Cr/Au film is successfully deposited onto the blazed grating surfaces to improve the diffracted power by a protective mask process. The displacements are measured by applying voltage to the microactuators, and optical experiments are performed to characterize the diffraction properties of the fabricated blazed gratings.

#105846 - $15.00 USD Received 6 Jan 2009; revised 20 Feb 2009; accepted 26 Feb 2009; published 4 Mar 2009

2. Theoretical approach

Figure 1(a) shows the cross sectional schematic diagram of the silicon pitch-variable blazed grating. The grating consists of silicon beams with a top surface blazed for the first order diffraction beam. The light is diffracted in different directions, and the directions of the light beam depend on the spacing of the grating and the wavelength of light so that the diffraction grating acts as a dispersive element. In case that the top surface of the beam is coated by a reflective metal film, the incident light on the beam is mostly reflected by the metal film at the blazed angle that corresponds to the first order beam. Here, the grating beam period is expressed by P and the width of each beam is denoted by a. The expansion of the freestanding grating beams is realized by the microactuators; hence, optical response can be tuned in response to a change in grating period P. The duty ratio d (=a/P) decreases with the increase of P. Since light is transmitted in the region between the grating beams, the duty ratio denotes the fraction of the light reflected by the grating. Increasing the duty ratio, the reflected light is expected to increase, but it becomes difficult to fabricate the narrow gap between the gratings. To the limit of d =1, the grating surface profile under stationary condition corresponds to that of a conventional blazed surface grating.

In the case that a reflective metal film coats the top surface of each beam, the grating works as a phase and amplitude grating with a binary reflectance. The reflectance of the grating is given by the equation,

$$R(x)=\begin{cases} A\exp(-2\pi iy/\lambda) & -a/2 \le x-nP \le a/2 \\ 0 & x-nP<-a/2\,,\quad a/2<x-nP \end{cases} (n=0,\pm 1,\pm 2,\pm 3\cdots) \tag{1}$$

where A is the reflectance of the coated metal film, λ is the wavelength, and y is the top surface profile of the grating and is given by,

$$y=-\frac{h}{a}x \tag{2}$$

where h is the blazed height of the blazed grating shown in Fig. 1(a). The intensity of each diffraction order beam is proportional to the Fourier expansion coefficient of the reflectance R under a plane wave incidence [10, 23, 24]. Therefore, the intensity in the k th order diffraction beam can be expressed as,

$$I(k)=\frac{C_0}{P}\int_{-P/2}^{P/2}R(x)\exp(-2\pi ikx/P)\,dx \tag{3}$$

where C_0 is a proportional constant. Introducing (1) and (2) into (3),

$$\begin{aligned} I(k) &= \frac{C_0A}{P}\int_{-a/2}^{a/2}\exp\left\{2\pi i\left(\frac{2h}{a\lambda}-\frac{k}{P}\right)x\right\}dx \\ &= C_0A\frac{\sin\left\{2\pi\left(\frac{2h}{a\lambda}-\frac{k}{P}\right)\frac{a}{2}\right\}}{\pi P\left(\frac{2h}{a\lambda}-\frac{k}{P}\right)} \end{aligned} \tag{4}$$

#105846 - $15.00 USD Received 6 Jan 2009; revised 20 Feb 2009; accepted 26 Feb 2009; published 4 Mar 2009

$$I(k=1) = C_0 A \frac{a}{P} \frac{\sin\left\{\pi\left(1-\frac{a}{P}\right)\right\}}{\pi\left(1-\frac{a}{P}\right)} \tag{5}$$

$$= C_0 A\, d\,\mathrm{sinc}\,(1\text{-}d)$$

In our work, continuous blazed profiles are approximated by 4-level stair steps as shown in Fig. 1(b). Gold film acting as the reflective material is deposited onto the blazed surface to improve the diffraction efficiency. Figure 1(c) shows the normalized diffraction efficiency *I(k)* in the first order as a function of the grating duty ratio *d*. For a continuous blazed grating, the normalized *I(k)* becomes unity at *d=1*, which corresponding the conventional blazed grating. Therefore, as is well known, for the conventional blazed grating without a pitch-variable mechanism, 100% blazed efficiency is obtained theoretically. For the planar-surface case shown in Fig.1(a), the grating functions as an amplitude grating and its efficiency is low. Compared to the planar-surface profile, the maximum blazed efficiency is greatly improved from 10.1% to 40.5%, 81.1% and 95% for 2-level, 4-level and 8-level blazed gratings, respectively. Due to the gap between the grating beams in the case of the pitch-variable grating, the loss of reflection cannot be avoidable. As shown in Fig. 1(c), the diffraction efficiency decreases faster than the linear decrease of the reflection area in response to a decrease in the duty ratio *d*. For a continuous blazed grating, the efficiency is equal to 0.32 at the duty ratio of 0.5. In the region of *d* higher than 0.8, the decrease in diffraction efficiency is relatively compared to the linear decrease of the reflection area. Therefore, the filling factor of the pitch-variable grating is designed to be 0.8, where the efficiency is 0.75.

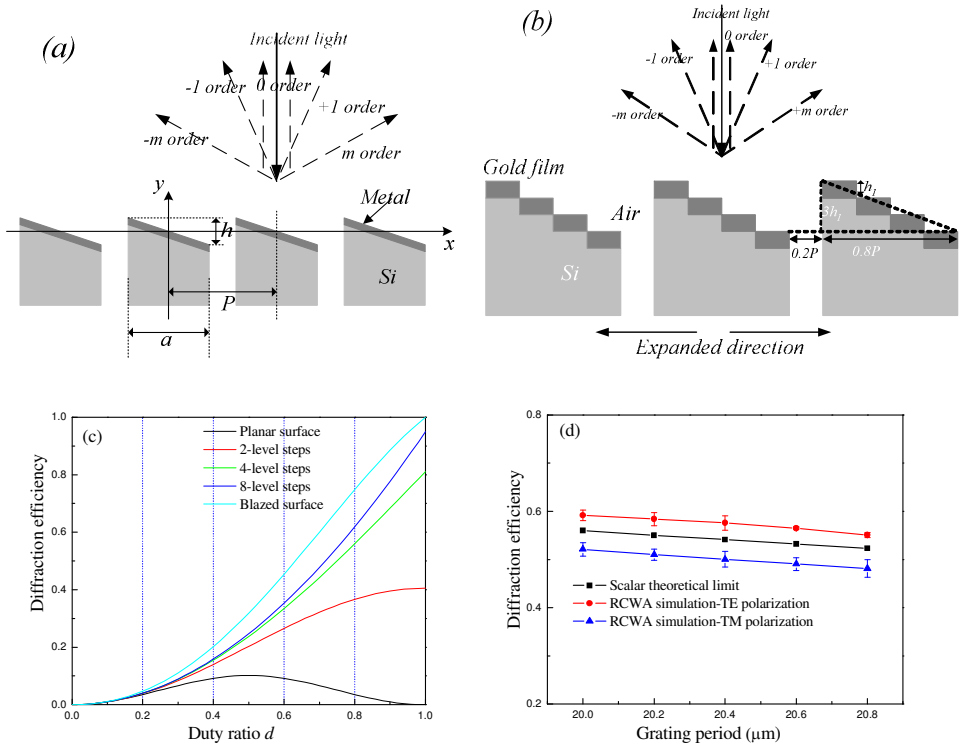

Fig. 1. (a)&(b) Schematic diagram of a pitch-variable blazed grating; (a) continuous blazed profile; (b) 4-level blazed profile; (c) the 1st order diffraction efficiency as a function of the grating duty ratio; (d) the 1st order diffraction efficiency of variable grating period calculated by RCWA.

#105846 - $15.00 USD Received 6 Jan 2009; revised 20 Feb 2009; accepted 26 Feb 2009; published 4 Mar 2009

The optical response of the 4-level blazed grating is also simulated by using the rigorous coupled-wave analysis (RCWA) method, which can provide more precise analysis compared to the scalar approximation. A commercial implementation (G-Solver) of the RCWA code is used for the simulations. The average diffraction efficiency versus the variable grating period is calculated in the range 1460nm~1580nm for the 1st diffraction order beam of transverse electric (TE) polarized incident light (the light is polarized parallel to the linear grating surface) and transverse magnetic (TM) polarized incident light (the light is polarized perpendicular to the linear grating surface), respectively. The grating period is 20μm, and the step height is 150nm, equal to the thickness of gold film. The devices are supported on a 10μm silicon device layer, and the initial separation trenches have a width of 4μm (d=0.8), larger than the target wavelength. Hence, approximately 20% of the light is lost due to the separation trenches. As shown in Fig.1(d), the average diffraction efficiency is around 0.592 under TE polarization and 0.521 under TM polarization, and the scalar theoretical limit is around 0.56, which doesn't take polarization into account. The scalar theoretical limit agrees well with the RCWA simulation results. The duty ratio d decreases when the grating is stretched. A relatively linear decrease in diffraction efficiency is observed in response to a small decrease in the duty ratio d. The diffraction efficiency does not change very much with an increase in grating period by the microactuator.

3. Device design and fabrication

One set of opposing electrostatic combdrive actuators are proposed to translate the freestanding grating beams, which are supported by the anchors, as shown in Fig.2(a). The anchors split the grating area into two symmetric parts. Here, the comb finger is 3μm wide, 10μm thick, and 45μm long and the gap between the comb fingers is 3μm. One pair of doubled folded springs is utilized in each microactuator, and the width b_s and the length L_s of the actuator spring are designed to be 3μm and 300μm, respectively. Adjacent grating beams are connected by the finger springs, and the width b_f and the length L_f of the finger spring are designed to be 3μm and 150μm, respectively. Thus, the calculated total stiffness is approximately 2.76N/m. The pitches of the designed gratings are 10, 12.5, 15, 17.5 and 20μm, respectively.

The pitch-variable 4-level blazed gratings are realized on a SOI wafer with a 10μm silicon device layer, 1μm buried oxide layer, and 200μm silicon handle layer. The 4-level blazed surface profile was defined by a two-mask process [20]. The top silicon was etched by FAB, which was performed with an etching rate of approximately 15nm/min at the high voltage of 2.0kV and the accelerated current of 20mA. The third mask was used to pattern the microactuators, finger springs, anchors and separation trenches, and the silicon device layer was etched down to the buried oxide layer by RIE. And then, the silicon handle layer was patterned from backside by photolithography. Deep RIE was used to etch through the silicon handle layer under movable part region, and the buried oxide layer acted as a definite etch stop. The freestanding structures were then generated by removing the remained buried oxide layer in vapor HF. Finally, a 5nm/150nm Cr/Au film was deposited onto the blazed grating surfaces by a protective mask process.

4. Experimental results and discussion

Figure 2 shows the scanning electron microscope (SEM) images of the freestanding tunable 4-level blazed grating. The Cr/Au film is successfully deposited onto the grating surfaces and no sticking problems are observed in the grating area, as shown in Fig. 2(a). It is noted that the silicon substrate is removed under the grating region to prevent reflection noise. The fabrication capability employed here has a minimum linewidth of 2μm, and the fabrication tolerance is improved in response to an increase in grating period. Fig. 2(b) and (c) illustrate the 20μm and 15μm blazed gratings respectively. Fig. 2(d) illustrates the cross-sectional view of 4-level blazed gratings fabricated on a referenced silicon wafer. The grating period is 10μm, and additional structures are found in the grating areas. The deviations between the profile generated in reality and the ideal element are caused by a small lateral misalignment in

#105846 - $15.00 USD Received 6 Jan 2009; revised 20 Feb 2009; accepted 26 Feb 2009; published 4 Mar 2009

multi-mask process. Such deviations from the ideal surface profile will result in a reduction of the diffraction efficiency in the desired signal orders.

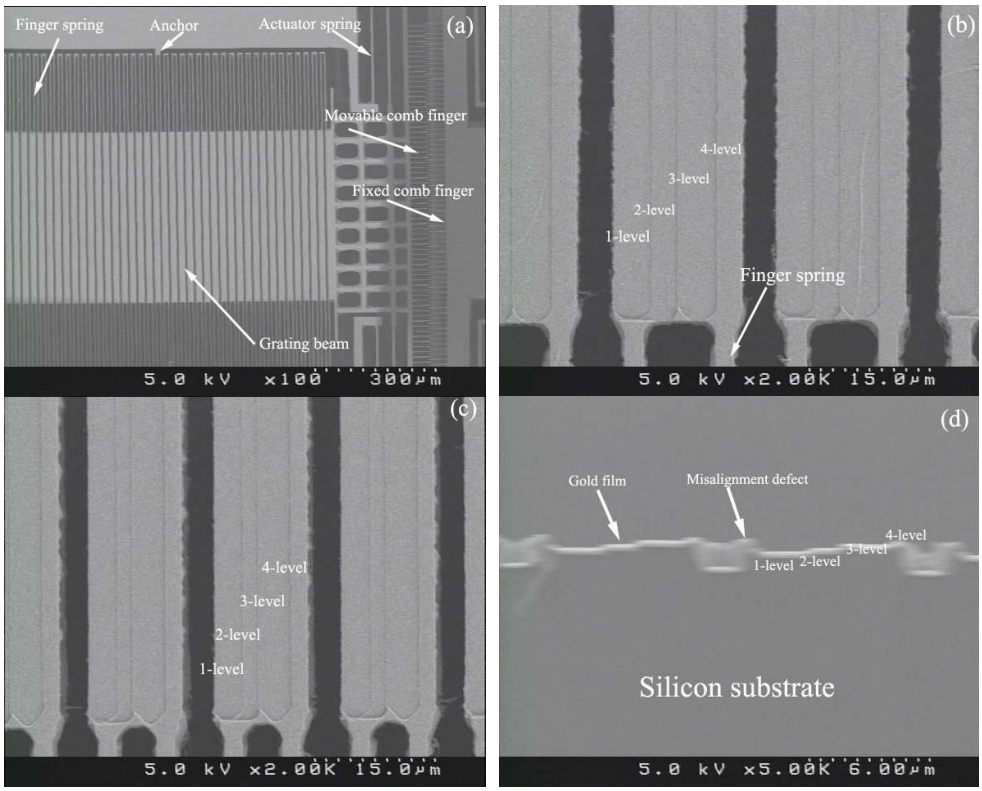

Fig. 2. SEM images of tunable freestanding 4-level blazed gratings. (a) the freestanding device; (b) the magnified view of 20μm period grating; (c) the magnified view of 15μm period grating; (d) the cross-sectional view of 4-level blazed gratings.

Pitch-variation of fabricated devices is characterized by applying voltage to the microactuators, and the displacement is observed under a microscope. Figure 3 shows optical images of the grating beams during driving. Fig. 3(a) shows the initial state and Fig. 3(b) shows the grating beams with 100V applied. The shift of the movable comb fingers results in a stretching of each grating. Based on the theoretical model, approximately 16μm shift can be achieved by applying 100V to the designed microactuators. The tuning range depends on grating period and grating number. For a 20μm period grating with grating number of 19, 0.84μm elongation in each grating can be realized; hence, the periodicity tuning (*(P(V)-P(0))/P(0)*) is about 4.2%, corresponding to a tuning range of 65nm at a wavelength of 1550nm. Though a little deviation can be observed between the measurement and the simulation (especially for high voltage), large displacement of movable comb finger is experimentally proven with high voltage applied as shown in Fig. 3(c). For a 20μm period grating, a relative tuning *(P(V)-P(0))/P(0)* of approximately 4% can be experimentally realized, higher than the reported 2.5% periodicity tuning [9]. The periodicity tuning can be greatly increased for blazed gratings with small period.

#105846 - $15.00 USD Received 6 Jan 2009; revised 20 Feb 2009; accepted 26 Feb 2009; published 4 Mar 2009

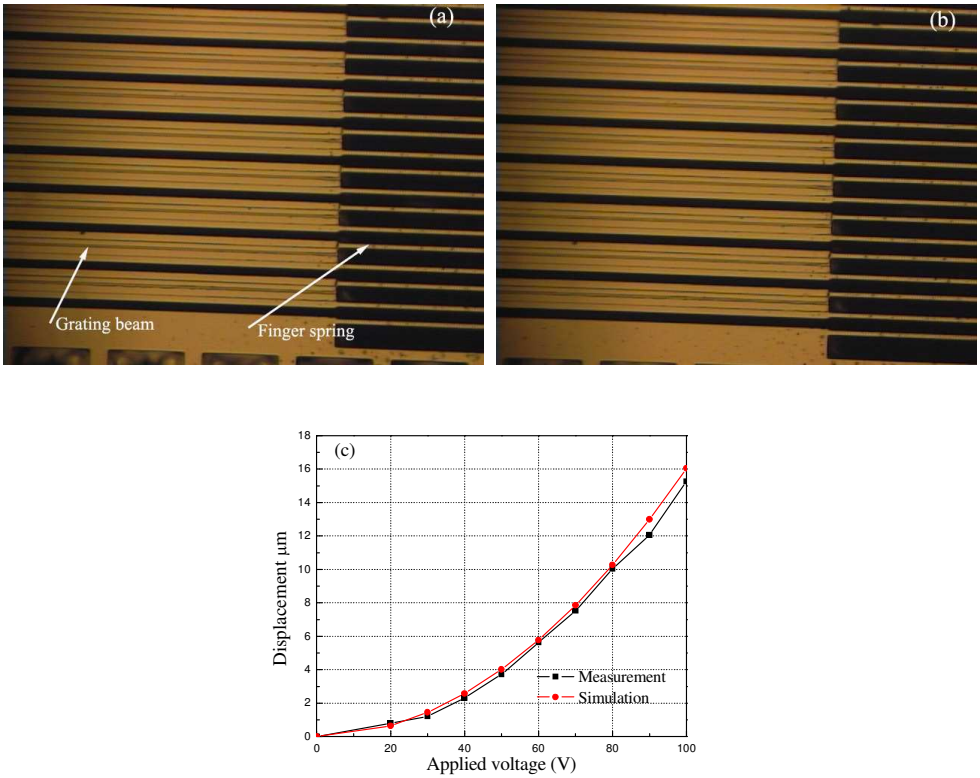

Fig. 3. (a) Optical images of the grating beam at the initial state; (b) with 100V applied; (c) Measured and simulated displacement versus applied voltage.

A beam of polarization controlled light from a tunable laser (Agilent 81682A) is used as the light source, and the 20μm period blazed grating is measured at a range of 1460nm~1580nm. Figure 4(a) shows the diffraction pattern as a function of wavelength, which is captured by an infrared camera. The diffracted power is mainly concentrated on the 1st diffraction order, which is also confirmed by the measured 1st diffraction efficiency. As shown in Fig. 4(b), the average diffraction efficiency is around 0.468 under TE polarization and around 0.402 under TM polarization, respectively. The experimental spectra are normalized to that of commercial gold mirror. The periodic ripple is caused by the fluctuation in measurement. Although the measured diffraction efficiency is lower than the calculated diffraction efficiency due to the fabrication deviations from the ideal 4-level blazed grating, the fabricated 4-level blazed gratings extend the diffraction efficiency of existing MEMS diffraction gratings, in which a 9.5% diffraction efficiency of the 1st diffraction order is reported with a planar-surface profile [5].

#105846 - $15.00 USD Received 6 Jan 2009; revised 20 Feb 2009; accepted 26 Feb 2009; published 4 Mar 2009

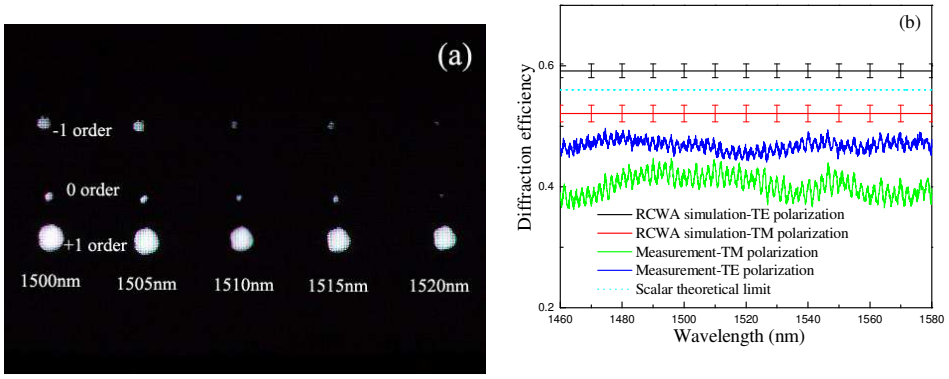

Fig. 4. (a) Diffraction pattern versus wavelength obtained from infrared camera; (b) Measured and simulated diffraction efficiency of 20μm period grating.

5. Conclusions

We described a SOI process for implementing the pitch-variable blazed grating in association with MEMS technology. The 4-level blazed surface profile is realized by combining a two-mask process with FAB etching. The freestanding grating beams and MEMS actuators are achieved on a 10μm silicon device layer, which can provide sufficient stiffness to the whole device. A Cr/Au film is successfully deposited onto the blazed grating surfaces to improve the diffracted power by a protective mask process. Mechanical response and diffraction efficiency of fabricated devices are characterized, and the experimental results indicate that the fabricated 4-level blazed gratings extend both the tuning range and the diffraction efficiency of the 1st diffraction order of present MEMS diffraction gratings.

Acknowledgments

This work was supported by the Research Project, Grant-In-Aid for Scientific Research(17068002).

#105846 - $15.00 USD Received 6 Jan 2009; revised 20 Feb 2009; accepted 26 Feb 2009; published 4 Mar 2009